New Journal of Physics
The open access journal at the forefront of physics

Deutsche Physikalische Gesellschaft DPG IOP Institute of Physics

PAPER • OPEN ACCESS

Stimulated Raman adiabatic passage with two-color x-ray pulses

To cite this article: Antonio Picón *et al* 2015 *New J. Phys.* **17** 083038

New Journal of Physics
The open access journal at the forefront of physics

Deutsche Physikalische Gesellschaft DPG
IOP Institute of Physics

Published in partnership with: Deutsche Physikalische Gesellschaft and the Institute of Physics

OPEN ACCESS

RECEIVED
8 May 2015

REVISED
1 July 2015

ACCEPTED FOR PUBLICATION
17 July 2015

PUBLISHED
19 August 2015

PAPER

Stimulated Raman adiabatic passage with two-color x-ray pulses

Antonio Picón[1], **Jordi Mompart**[2] **and Stephen H Southworth**[1]

[1] Argonne National Laboratory, Argonne, Illinois 60439, USA
[2] Departament de Física, Universitat Autònoma de Barcelona, E-08193 Bellaterra, Spain

E-mail: apicon@anl.gov

Keywords: XFEL, STIRAP, quantum control

Abstract

Recent techniques in x-ray free electron lasers allow the generation of highly coherent, intense x-ray pulses with time lengths on the order of femtoseconds. Here we explore the possibilities of using such x-ray pulses to control matter based on coherence. In particular we propose a theoretical scheme to perform stimulated Raman adiabatic passage in the x-ray regime by using inner-hole excited states. Numerical results in two well-known systems, the neon atom and the carbon monoxide molecule, show a robust control of population transfer. In the molecule, vibrational selectivity is achieved with femtosecond x-ray pulses. This work supports the possibility of using two-color x-ray pulses for coherent control.

1. Introduction

There is an enormous effort and worldwide interest to develop x-ray free electron lasers (XFELs) as sources of intense, short duration, and highly coherent x-ray pulses. In the optical regime coherence enables the application of quantum control techniques that have not yet been exploited in the x-ray regime. The extension of quantum control techniques to high photon energies allows the combination of powerful techniques to control population with the characteristic site-specificity of the x rays. Here we demonstrate theoretically a scheme based on stimulated Raman adiabatic passage (STIRAP) using x rays for an efficient control of population transfer. In spite of the rapid decay of the $1s^{-1}3p$ inner-hole excited state in atomic neon, we achieve 30% of population transfer. Furthermore, we observe vibrational selectivity in molecular carbon monoxide using the oxygen $1s \rightarrow 2\pi$ vibronic manifold intermediate states.

First experiments using XFEL pulses in atoms, molecules, and clusters [1–3] show a complex multiphoton response driven by strong electron correlation, as matter under the absorption of an x-ray photon will be excited into an inner-shell hole state that rapidly decays on the timescale of a few femtoseconds to hundreds of attoseconds either by an Auger process or by a fluorescent process, and inner-hole decays proceed concurrently with the absorption of additional x-ray photons. Hence, the typical response to XFEL pulses is to produce highly charged final states, and the extension of coherent quantum control techniques to the x-ray regime is not trivial. However, recent developments in seeding techniques at XFELs [4–7] have significantly increased the quality of the pulse temporal coherence. In the optical regime, in which lasers have achieved a high-degree of spatio-temporal coherence several decades ago, we find many quantum control techniques for atoms and molecules based on coherence [8].

In this work, STIRAP, a well-established coherent control technique routinely used to produce population transfer between two quantum states [9, 10], is extended from the optical to the x-ray regime. The advantage of STIRAP is that during the transfer, the population in the intermediate inner-hole state is highly suppressed and avoids radiation damage.

We study both an atomic and a molecular system, in particular a scheme for the neon atom and for the carbon monoxide molecule. Numerical simulations show positive results of this technique in both systems, supporting then the possibility of controlling matter by fully exploiting the temporal coherence of x-ray pulses.

In STIRAP the dynamics of a system interacting with two pulses is mainly confined in three quantum states, and the effective hamiltonian as a result of the projection onto these states is a good approximation. The essential

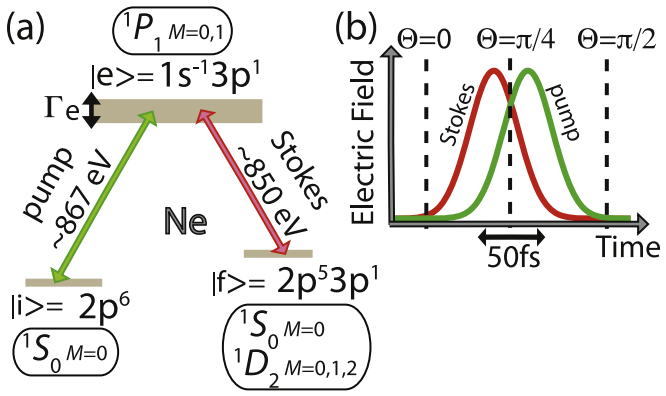

Figure 1. (a) STIRAP scheme for neon, the three main states are shown. See text for further details. (b) Typical scheme for STIRAP, Stokes pulse arrives to the atomic system before the pump pulse.

concept in STIRAP is that the change of the pulses in time is smooth enough, and the system evolves following an eigenstate of the hamiltonian. Hence, the dynamics is adiabatically driven. We use a three-level-lambda system as in figure 1(a), in which the pump pulse couples the initial state $|i\rangle$ with the intermediate state $|e\rangle$, while the Stokes pulse couples the intermediate state with the final state $|f\rangle$. In the two-photon resonance condition one eigenstate is given by the so-called dark state $|\psi\rangle = \cos\Theta|i\rangle - \sin\Theta|f\rangle$ [9], where the parameter Θ is given by the ratio $\tan\Theta = \Omega_P/\Omega_S$, where $\Omega_{P/S}$ is the corresponding Rabi frequency of each pulse (the dipole moment of the transition times the envelope of the electric field). Hence, in a scheme in which two overlapping pulses are slightly delayed in time as in figure 1(b) and the dynamics is adiabatically driven, the parameter Θ smoothly changes from 0 to $\pi/2$ and all the population initially located in the initial state $|i\rangle$ will be transferred to the final state $|f\rangle$ without populating the intermediate state $|e\rangle$. STIRAP has been applied to numerous physical scenarios in the optical regime not only to transfer atomic and molecular population between two internal levels but also to generate single photons on demand [11], create ultracold molecules [12], for quantum information purposes [13], and to manipulate the external degrees of freedom of matter waves [14].

2. Theoretical model

In order to describe the time evolution of the neon atom under the interaction of the two x-ray pulses, we use a similar theoretical model used in previous works [18–20] by solving the equations of motion

$$\begin{aligned}
\mathrm{i}\,\dot{a}_i(t) &= \left[E_i - \mathrm{i}\frac{\Gamma_{ix}(t)}{2}\right]a_i(t) + \mu_{ie}\varepsilon_x(t)a_e(t)\,,\\
\mathrm{i}\,\dot{a}_e(t) &= \left[E_e - \mathrm{i}\frac{\Gamma_e + \Gamma_{ex}(t)}{2}\right]a_e(t)\\
&\quad + \mu_{ei}\varepsilon_x(t)a_i(t) + \mu_{ef}\varepsilon_x(t)a_f(t)\,,\\
\mathrm{i}\,\dot{a}_f(t) &= \left[E_f - \mathrm{i}\frac{\Gamma_{fx}(t)}{2}\right]a_f(t) + \mu_{fe}\varepsilon_x(t)a_e(t)\,,
\end{aligned} \tag{1}$$

where we have assumed the ansatz that the system is described by the wavefunction $|\psi\rangle = a_i(t)|i\rangle + a_e(t)|e\rangle + a_f(t)|f\rangle + \sum_n \int \mathrm{d}E_a\, b_n(E_a, t)|E_a, n\rangle$, where $|E_a, n\rangle$ is a final state after the inner-hole decay, either a state after an Auger process or a fluorescence process. $\varepsilon_x(t) = \varepsilon_P(t) + \varepsilon_S(t)$ is the sum of the electric field of the two pulses, and μ_{ab} is the dipole transition between state a and b given by $\mu_{ab} = \langle a|\sum_j \mathbf{r}_j \cdot \mathbf{e}_x|b\rangle$, where $\mathbf{r}_j$ is the position operator of electron j and $\mathbf{e}_x$ is the polarization vector of the x rays. Here we only consider linearly polarized pulses with parallel polarization. E_i, E_e, and E_f are the energies of the initial, intermediate, and final state respectively. The inner-hole decay of the intermediate state is represented by the gamma parameter $\Gamma_e = \Gamma_a + \Gamma_f$, where Γ_a represents the decay through Auger processes and Γ_f thorough fluorescence [21, 22]. Γ_{ax} describes the valence ionization of 2s and 2p electrons in state a within the Markov approximation [23], and it can be expressed as $\Gamma_{ax} = \sigma_a J_x(t)$, where $J_x(t)$ is the instantaneous x-ray flux [24, 25], and σ_a is the x-ray photoionization cross-section. We have calculated all the parameters we need with Cowan's Hartree–Fock program [26, 27], besides the inner-hole decay width taken from [15] to be around $\Gamma_e = 0.27$ eV (Auger processes are dominant, mainly 99% in neon).

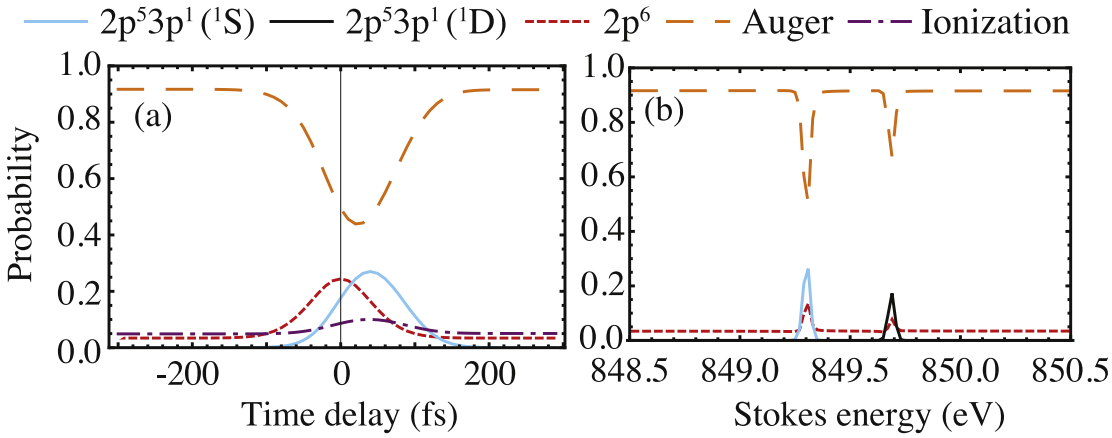

Figure 2. Population probabilities for $2p^53p^1(^1S_0)$ (light solid line, blue color), $2p^53p^1(^1D_2)$ (black solid line), ground state (dotted line), Auger decay yield (dashed line), and ionization yield (dotted–dashed line) when (a) we change time delays between pump and Stokes pulse, pump photon energy at 867.47 eV and Stokes photon energy at 849.31 eV, and (b) we change photon energies of the Stokes pulse, pump photon energy fixed at 867.47 eV. Both pulses have a temporal Gaussian profile of 83 fs with FWHM in intensity, pump intensity 1×10^{16} W cm^{-2}, and Stokes intensity 1×10^{14} W cm^{-2}.

The theoretical model used for the molecule is similar to the atomic one. In our ansatz we project the wavefunction into the main electronic levels, $\Psi(\mathbf{X}, R, t) = a_i(R, t)\Phi_i(\mathbf{X}, R) + a_e(R, t)\Phi_e(\mathbf{X}, R) + a_f(R, t)\Phi_f(\mathbf{X}, R) + \sum_n \int dE_a b_n(E_a, R, t)\Phi_{E_a,n}(\mathbf{X}, R)$, where $\mathbf{X}$ stands for the electronic coordinates and R is the internuclear distance between carbon and oxygen atoms. Hence, the main difference with the atomic case is that the amplitudes now are R dependent (they are nuclear wavepackets propagating in the corresponding electronic levels). Following the same procedure used to derive the equations of motion (1), we obtain similar equations for the molecule within the Born–Oppenheimer approximation, in which the energies are changed by the kinetic energy operators of the nuclear wavepacket plus the electronic potential energy surfaces (PES). The gamma parameters and the dipole moments are also R dependent, but this dependency can be neglected in the range of internuclear distances where the main dynamics is. PES are obtained from spectroscopic data [28, 29] and dipole moments are calculated with CFOUR at the level of EOM-CCSD/aug-cc-pVDZ [30].

3. Neon atom

In figure 1(a) we present a three-level-lambda system in the soft x-ray regime for a neon atom, in which state $|i\rangle$ is the ground state of neon, the intermediate state $|e\rangle$ is the inner-hole state $1s^{-1}3p$, and the state $|f\rangle$ is the final state with electron configuration $2p^53p^1$. The inner-hole state lifetime is very short, around 2.4 fs [15], therefore any population in the intermediate state decays very fast mainly through an Auger process. A simple rule to drive STIRAP is that the adiabaticity factor $\alpha = \sqrt{\Omega_P^2 + \Omega_S^2}\ \Delta T$ has to be large, i.e. $\alpha \gg 1$, where ΔT is the time period in which the two pulses overlap. However, when the intermediate state has a strong decay the population transfer is less efficient [16]. In that case we expect that the population transfer is still high if additionally it is satisfied that $\alpha^2 \gg \Gamma_e \Delta T$, where Γ_e is the inner-hole decay rate. Naturally, we avoid the effects of the strong inner-hole decay if we increase the (intensity) Rabi frequency, but in a real system we need to account for ionization, in the case of the neon atom for L-shell ionization, that limits the intensity. A similar scheme has been studied in the UV regime with autoionizing states, and in that regime ionization cross sections are so large that the pulses end up ionizing the system before any population transfer occurs [17]. The ionization scales as $\propto \alpha^2/\Delta T$, so there is a trade off between population transfer and ionization. Therefore, it is not obvious that STIRAP can be performed in the x-ray regime.

The ground state $^1S_0$ is taken as reference, i.e. $E_i = 0$ eV, and the excited inner-hole state $^1P_1$ is at $E_e = 867.47$ eV. The accessible final state $|f\rangle$ can be at the state $^1S_0$ or $^1D_2$, with slightly different energies $E_f^{(S)} = 18.16$ eV and $E_f^{(D)} = 17.78$ eV, respectively. In the LS coupling, if both pump pulse and Stokes pulse are linearly polarized and parallel, the angular moment M must be conserved $\Delta M = 0$. In figure 2(a) we show our numerical simulations for a pump and a Stokes pulse with Gaussian profiles, with FWHM in intensity of 83 fs, and photon energies of 867.47 and 849.31 eV, respectively. Because the dipole moment μ_{ef} is around 10 times larger than μ_{ei}, we found that the best scheme to achieve population transfer is that the transitions have similar Rabi frequency, i.e. the pump electric field should be 10 times larger than the Stokes electric field (in intensity around 100 times larger). We use 10^{16} W cm^{-2} intensity for the pump pulse (2.5 μJ energy per pulse) and

10^{14} W cm^{-2} intensity for the Stokes pulse (0.12 μJ energy per pulse). Results of figure 2(a) show a significant effect when we change the time delay of both pulses. For long negative time delays, the pump pulse arrives first and excites most of the population to the inner-hole state that decays mainly by an Auger process, and we observe around 90% of Auger decay yield. At these intensities we start to observe a strong L-shell ionization of 5%. For long time delays, in which the Stokes pulse arrives first to the atom, similar behavior is observed with respect to long negative time delays. Here though we observe an almost unnoticeable reduction of 0.1% of the Auger decay yield as the Stokes pulse starts ionizing the system before the arrival of the pump pulse that is much more intense. Strong population transfers are observed when both pulses are overlapping. When the time delay is positive, that means that the Stokes pulse arrives first to the atom, then we observe a large population transfer, with the maximum population transfer to $2p^5 3p^1(^1S_0)$ of almost 30% at the time delay around 50 fs. Population transfer happens in a very short time window, around 200 fs, while outside that time window no transfer to $2p^5 3p^1(^1S_0)$ is observed. The population transfer is less than expected due to the strong inner-hole decay rate. If the inner-shell decay rate was negligible, we achieve almost 90% population transfer. Our adiabaticity factor is $\alpha \sim 9$ and $\alpha^2/\Gamma_e \Delta T \sim 3$. We also observe an increase of the ground state population, which is the signature of the so-called *quantum overdamping* effect characteristic of three-level systems with strong decay in the intermediate state, in which the system shows up as effectively decoupled from the external field. This effect decreases if $\alpha^2/\Gamma_e \Delta T$ increases. We also note the huge decrease of Auger decay yield when there is an increase of population of the ground state and the final state $2p^5 3p^1$. This is understood as the population in the inner-hole state being small, so the Auger decay yield is highly suppressed in spite of the short lifetime (2.4 fs), and most of the population stays in bound states, increasing then the contribution of L-shell ionization. In figure 2(b) we fix the time delay of the two pulses to 50 fs and we change the photon energy of the Stokes pulse. We observe the STIRAP in very narrow windows of photon energies of 0.1 eV around the resonance transition 849.31 eV for $2p^5 3p^1(^1S_0)$ and 849.69 eV for $2p^5 3p^1(^1D_2)$. In conclusion, we observe a significant STIRAP mechanism in spite of the strong Auger decay rate. We also checked that when the final state $2p^5 3p^1$ is coupled by the pump pulse to the inner-hole state $1s^{-1}2p^5 3p^2$ (these states are between 883 and 887 eV), there are no major effects, so that coupling can be neglected.

4. Carbon monoxide molecule

In a molecule, naturally, defining a three-level system for x-ray STIRAP may be difficult mainly due to the vibrational manifold [31], not only because of the manifold of the initial and final states, but also of the inner-hole state. The question of selectively transferring population from one vibrational state to another vibrational state in a molecule goes back to the origins of STIRAP [32, 33]. In order to show the selectivity of x-ray STIRAP in a molecule, we model the CO molecule as an example of the feasibility of the method.

The electron configuration of CO in its ground state is $(1\sigma^2)\,(2\sigma^2)\,(3\sigma^2)\,(4\sigma^2)\,(1\pi^2)\,(5\sigma^2)\ X\ ^1\Sigma^+$. CO has a strong resonance at the oxygen K-edge due to the resonant excitation O 1s $\rightarrow$ LUMO (2π). Obviously, this transition is only possible if the LUMO has a nonzero density on the oxygen site. This resonance has been extensively studied in XAS measurements [34, 35], where it is shown that the vibrational manifold of the transition is broad and encompasses $v = 0$ to $v = 10$ in the range 533–536 eV. The strength of the excitation observed in XAS is related to the Frank–Condon factors of the excited vibrational states with the ro-vibrational ground state, and it also depends on the orientation of the molecular axis (MA) with respect to the x-ray polarization. In particular, we need a component of the polarization perpendicular to the MA to induce the excitation, i.e. angle $\theta = 90°$, see inset figure 3(b). Another interesting point is the relation of x-ray STIRAP with resonant inelastic x-ray scattering (RIXS). In STIRAP, the transition driven by the Stokes pulse is stimulated, while in RIXS the transition is due to spontaneous emission. RIXS spectra depend on the dipole transitions from inner-hole states to final states, and in molecules RIXS is used to study vibronic properties of inner-hole levels [36, 37]. From RIXS measurements we can extract the final states with the strongest dipole transitions from the inner-hole $(O1s)^{-1}2\pi$ state [38]. For simplicity we only include the three main final states with stronger dipole transitions in the theoretical model; $(5\sigma)^{-1}2\pi\ ^1\Pi$, $(1\pi)^{-1}2\pi\ ^1\Sigma^-$, and $(1\pi)^{-1}2\pi\ ^1\Delta$, see figure 3(a). Transition $(O1s)^{-1}2\pi \rightarrow (5\sigma)^{-1}2\pi$ is only possible for a component of the electric field along the MA, whereas transitions $(O1s)^{-1}2\pi \rightarrow (1\pi)^{-1}2\pi$ are only possible for components of the electric field perpendicular to the MA. This angular dependence is important for STIRAP.

The selectivity of the population transfer depends on the bandwidth of the pulses. In our case, gaussian pulses with FWHM of 83 fs, the bandwidths are sufficient for the initial and final vibrational manifold. However, the $(O1s)^{-1}2\pi$ state has a short lifetime of 3.6 fs, i.e. a natural linewidth of 0.18 eV, and the energy gap between neighboring vibrational states is similar to the natural linewidth, so the pump excitation unavoidably populates several vibrational states and decreases the efficiency of the population transfer. On the other hand, the dipole moments of the resonances are one order of magnitude larger than in neon, but the ionization cross sections are

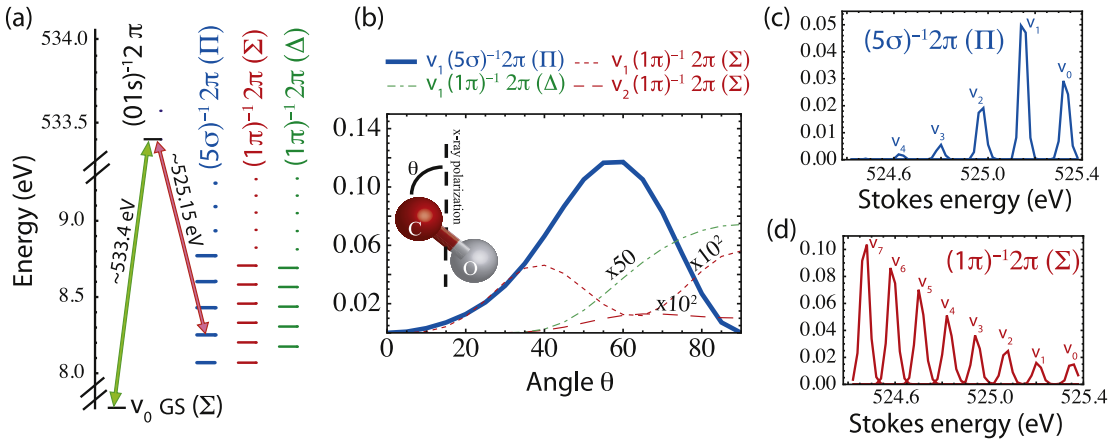

Figure 3. (a) Vibrational manifold of the main electronic levels involved in the dynamics. (b) Angular dependence of the population transfer to different final states using photon energies 533.4 and 525.15 eV for pump and Stokes pulse respectively. θ is the angle between molecular axis and x-ray polarization. (c) and (d) Vibrational excitation to the electronic levels $(5\sigma)^{-1}2\pi$ $^1\Pi$ and $(1\pi)^{-1}2\pi$ $^1\Sigma$ respectively averaged over the angular dependence shown in (b). We use different Stokes photon energies for a fixed pump photon energy at 533.4 eV. Both pulses are Gaussian with FWHM of 83 fs, pump intensity 5×10^{14} W cm^{-2}, and Stokes intensity 1×10^{15} W cm^{-2}.

roughly two orders of magnitude larger due to the contribution of the K-shell ionization of carbon. Despite these large cross sections, we observe efficiencies larger than 10% in figure 3(b). We use the three-level system defined by the GS-v_0 state, (O1s) $^{-1}2\pi$-v_0 state, and $(5\sigma)^{-1}2\pi$-v_1 state, in which the final $(5\sigma)^{-1}2\pi$-v_1 state is well separated in energy from other neighboring vibrational states. We show in figure 3(b) that the main population transfer is to the $(5\sigma)^{-1}2\pi$-v_1 state, demonstrating the strong selectivity of the final vibrational state with few-femtosecond pulses. We also show the dependence of the population transfer on the θ-angle. As expected, for angles midway between 0° and 90° we have the maximum transfer to the $(5\sigma)^{-1}2\pi$-v_1 state (to drive the pump transition, a component of polarization perpendicular to the MA is needed, and to drive the Stokes transition a component of polarization along the MA is needed). In order to induce transfer to other final vibrational states we change the Stokes photon energy. In figures 3(c) and (d) we show the population transfer into the vibrational states of $(5\sigma)^{-1}2\pi$ $^1\Pi$ and $(1\pi)^{-1}2\pi$ $^1\Sigma$ respectively for different photon energies. The population transfer depends on the Frank–Condon factors between the (O1s) $^{-1}2\pi$-v_0 state and the final vibrational states. If we change the pump excitation, then we obtain different population transfers. Hence, with x-ray STIRAP we have also access to nuclear properties of the inner-hole state. Here we assume that the molecule is a gas-phase target with random orientation, so we average over the angle θ for the results presented in figures 3(c) and (d). We should remark that, for our system, the intensities of the x-ray pulses are not high enough to observe nonadiabatic effects [39, 40]. In very high-intensity pulses, light-induced nonadiabatic effects can strongly couple electronic, vibrational, and rotational degrees of freedom.

5. Advantages and experimental feasibility of the control scheme

STIRAP is a robust control against intensity variations. This is an important feature for molecules whose resonances depend on the orientation of the molecule, as we showed for carbon monoxide. We note in figure 3(b) that for a wide range of angles we have still a significant transfer. That is the reason that in a gas- or liquid- phase experiment, in which the molecule is not oriented, we still obtain a significant population transfer. Compare for example the scenario of an ideally oriented molecule at 60° in figure 3(b) (around 10%) with a non oriented molecule in figure 3(c) (around 5%). Other control schemes based on resonant excitations, such as a $\pi + \pi$ pulse configuration, are sensitive to molecular orientation.

The robustness against intensity variations is very practical for XFELs experiments. The capabilities to produce two-color x-ray pulses at XFELs has improved very rapidly in the recent years. An interesting setup that may be suitable for performing x-ray STIRAP was recently reported in [41]. Using this setup, two-color seeded pulses can be generated in the hard-x-ray regime. STIRAP can be extended to this regime. However, there are some general concerns about using seeded pulses for STIRAP. The first concern is the temporal coherence of the pulses because seeded pulses are not perfectly Fourier transform limited. The adiabaticity condition is difficult to achieve and the efficiency is reduced. Hence, it will be difficult to drive STIRAP by using self-amplified spontaneous emission pulses. However, for near Fourier-transform limited pulses (seeded pulses), STIRAP is still possible by increasing the intensity of the pulses [42]. The second major concern is the strong shot-to-shot

variation of pulse intensities. Although STIRAP is less sensitive to pulse intensity fluctuations, very strong fluctuations could reduce the efficiency of the scheme. In any case, a shot-to-shot diagnosis and *a posteriori* selection of the experimental data can reduce these two problems [43].

We also remark that new schemes for performing population transfer in the XUV regime with a single pulse have been proposed [44]. It would be very interesting to study their feasibility in the x-ray regime avoiding the technical problem of generating two-color seeded pulses.

STIRAP keeps the population in the inner-excited state low and reduces the radiation damage. Other coherent control schemes based on the Brumer–Shapiro phase-control technique [45, 46] or the Tannor–Kosloff–Rice pump–dump technique [47, 48] are more challenging to implement in the x-ray regime due to the fast decay of the inner-hole state. Brumer–Shapiro phase-control techniques are based on interferences between multiphoton pathways, and Tannor–Kosloff–Rice pump–dump techniques are based on interferences between pathways due to the intrinsic evolution of excited states induced by the pump. Any scheme based on those techniques needs to have additional constraints on the time-dependent population of inner-hole states.

The STIRAP with two x rays may be very effective to induce excitations in the XUV/UV regime. We may wonder what is the advantage of the x-ray STIRAP versus a control scheme that uses XUV/UV pulses, such as techniques where the shaping of the pulses is required [49–51]. Certainly, two x rays give more flexibility to select an excitation in a localized site of a molecule by exploiting the characteristic site-specificity of the x rays. But x rays also offer longer penetration lengths compared with UV light and could be of special interest for liquid-phase experiments or buried interfaces of materials.

6. Conclusions

In conclusion, we have presented theoretical calculations for producing population transfer between two quantum states by exploiting coherent x-ray pulses. The scheme is based on the well-known STIRAP technique. Calculations are performed for the neon atom and the carbon monoxide molecule. In the molecule, few-femtosecond pulses allow the excitation of selected vibrational states satisfying the two-photon condition within the bandwidth of the pulses. We anticipate that the scheme works better for atomic and molecular systems that present strong resonances in the x-ray absorption spectrum with respect to the underlying continuum. This work suggests the use of XFEL pulses in a novel way for controlling matter, using inner-hole states but avoiding directly populating them. This approach is in contrast with other schemes that make use of inner-shell resonances such as Stimulated RIXS [52–54]. For the proposed STIRAP scheme, two-color high-intensity x-ray pulses are required, both of them having high temporal coherence (near Fourier-transform limited pulses).

Acknowledgments

We acknowledge discussions with L Cheng about calculating dipole transitions with CFOUR and R W Dunford about metastable states in neon. We also acknowledge fruitful discussions with P Bucksbaum, W Jakubetz, D Moonshiram, P Ho, G Doumy, C S Lehmann, A Zholents, A Marinelli, A Lutman, and C Bostedt, and the financial support of the US Department of Energy, Basic Energy Sciences, Office of Science, under contract # DE-AC02-06CH11357.

References

[1] Young L *et al* 2010 *Nature* **466** 56
[2] Hoener M *et al* 2010 *Phys. Rev. Lett.* **104** 253002
[3] Schorb S *et al* 2012 *Phys. Rev. Lett.* **108** 233401
[4] Amann J *et al* 2012 *Nat. Photonics* **6** 59
[5] Allaria E *et al* 2012 *Nat. Photonics* **6** 699
[6] Allaria E *et al* 2013 *Nat. Photonics* **7** 913
[7] Hemsing E, Stupakov G, Xiang D and Zholents A 2014 *Rev. Mod. Phys.* **86** 897
[8] Shapiro M and Brumer P 2006 *Phys. Rep.* **425** 195
[9] Bergmann K, Theuer H and Shore B W 1998 *Rev. Mod. Phys.* **70** 1003
[10] Bergmann K, Vitanov N V and Shore B W 2015 *J. Chem. Phys.* **142** 170901
[11] Kuhn A, Hennrich M and Rempe G 2002 *Phys. Rev. Lett* **89** 067901
[12] Takekoshi T, Reichsöllner L, Schindewolf A, Hutson J M, le Sueur C R, Dulieu O, Ferlaino F, Grimm R and Nägerl H-C 2014 *Phys. Rev. Lett.* **113** 205301
[13] Møller D, Madsen L B and Mølmer K 2008 *Phys. Rev. Lett.* **100** 170504
[14] Eckert K, Lewenstein M, Corbalán R, Birkl G, Ertmer W and Mompart J 2004 *Phys. Rev.* A **70** 023606
[15] Coreno M *et al* 1999 *Phys. Rev.* A **59** 2494
[16] Vitanov N V and Stenholm S 1997 *Phys. Rev.* A **56** 1463
[17] Li X, McCurdy C W and Haxton D J 2014 *Phys. Rev.* A **89** 031404

[18] Nina Rohringer and Santra Robin 2008 *Phys. Rev.* A **77** 053404
[19] Picón A, Buth C, Doumy G, Krässig B, Young L and Southworth S H 2013 *Phys. Rev.* A **87** 013432
[20] Picón A, Ho P J, Doumy G and Southworth S H 2013 *New J. Phys.* **15** 083057
[21] Weisskopf V F and Wigner E P 1930 *Z. Phys.* **63** 54
[22] Buth C and Schafer K J 2009 *Phys. Rev.* A **80** 033410
[23] Knight P L, Lauder M A and Dalton B J 1990 *Phys. Rep.* **190** 1
[24] Als-Nielsen J and McMorrow D 2001 *Elements of Modern X-ray Physics* (New York: Wiley)
[25] Buth C and Santra R 2007 *Phys. Rev.* A **75** 033412
[26] Cowan R D 1981 *The Theory of Atomic Structure and Spectra (Los Alamos Series in Basic and Applied Sciences)* (Berkeley: University of California Press)
[27] Los Alamos National Laboratory, Atomic Physics Codes http://aphysics2.lanl.gov/tempweb/lanl/
[28] Huber K P and Herzberg G 1979 *Molecular Spectra and Molecular Structure IV* (New York: Van Nostrand Reinhold)
[29] Correia N, Flores-Riveros A, Ågren H, Helenelund K, Asplund L and Gelius U 1985 *J. Chem. Phys.* **83** 2035
[30] CFOUR, Coupled-Cluster techniques for Computational Chemistry, a quantum chemical program package by Stanton J F, Gauss J , Harding M E, Szalay P G with contributions from Auer A A *et al* and the integral packages MOLECULE (Alml öf J and Taylor P R), PROPS (Taylor P R), ABACUS (Helgaker T, Jensen H J A , Jørgensen P, and Olsen J), and ECP routines by Mitin A V and van C Wüllen . For the current version, see http://cfour.de
[31] Coulston G W and Bergmann K 1991 *J. Chem. Phys.* **96** 3467
[32] Gaubatz U, Rudecki P, Schiemann S and Bergmann K 1990 *J. Chem. Phys.* **92** 5363
[33] Schiemann S, Kuhn A, Steuerwald S and Bergmann K 1993 *Phys. Rev. Lett.* **71** 3637
[34] Püttner R, Dominguez I, Morgan T J, Cisneros C, Fink R F, Rotenberg E, Warwick T, Domke M, Kaindl G and Schlachter A S 1999 *Phys. Rev.* A **59** 3415
[35] Adachi J, Kosugi N and Yagishita A 2005 *J. Phys. B: At. Mol. Opt. Phys.* **38** 127–52
[36] Hennies F *et al* 2010 *Phys. Rev. Lett.* **104** 193002
[37] Pietzsch A *et al* 2011 *Phys. Rev. Lett.* **106** 153004
[38] Skytt P, Glans P, Gunnelin K, Guo J and Nordgren J 1997 *Phys. Rev.* A **55** 146
[39] Cederbaum L S, Chiang Y C, Demekhin P V and Moiseyev N 2011 *Phys. Rev. Lett.* **106** 123001
[40] Demekhin P V and Cederbaum L S 2013 *J. Phys. B: At. Mol. Opt. Phys.* **46** 164008
[41] Marinelli A *et al* 2015 *Nat. Commun.* **6** 6369
[42] Kuhn A *et al* 1992 *J. Chem. Phys.* **95** 4215
[43] Marinelli A and Bostedt C 2015 private communication
[44] Demekhin P V and Cederbaum L S 2015 *Phys. Rev.* A **91** 013417
[45] Shapiro M and Brumer P 2003 *Principles of Quantum Control of Molecular Processes* (New York: Wiley)
[46] Brumer P and Shapiro M 1986 *Chem. Phys. Lett.* **126** 541
[47] Tannor D J and Rice S A 1985 *J. Chem. Phys.* **83** 5013
[48] Tannor D J, Kosloff R and Rice S A 1986 *J. Chem. Phys.* **85** 5805
[49] Pfeifer T *et al* 2007 *Opt. Express* **15** 3409
[50] Michael Hofstetter *et al* 2011 *Opt. Express* **19** 1767
[51] Austin D R and Biegert J 2014 *New J. Phys.* **16** 113011
[52] Weninger C *et al* 2013 *Phys. Rev. Lett.* **111** 233902
[53] Kimberg V and Rohringer N 2013 *Phys. Rev. Lett.* **110** 043901
[54] Beye M *et al* 2013 *Nature* **501** 191